DALTON
FULL PAPER

Syntheses, characterization and third order non-linear optical properties of the ruthenium(II) complexes containing 2-phenylimidazo[4,5-*f*][1,10]phenanthroline derivatives †

Hui Chao,[a] Run-Hua Li,[b] Bao-Hui Ye,[a] Hong Li,[a] Xiao-Long Feng,[c] Ji-Wen Cai,[c] Jian-Ying Zhou[b] and Liang-Nian Ji*[a]

[a] *Department of Chemistry, Zhongshan University, Guangzhou 510275, P. R. China. E-mail: cesjln@zsu.edu.cn*
[b] *State Key Laboratory of Ultrafast Laser Spectroscopy, Zhongshan University, Guangzhou 510275, P. R. China*
[c] *Center of Analysis and Determination, Zhongshan University, Guangzhou 510275, P. R. China*

Received 19th July 1999, Accepted 8th September 1999

The ruthenium(II) complexes $[Ru(dmb)_2(LH)][ClO_4]_2$ [dmb = 4,4′-dimethyl-2,2′-bipyridine; LH = 2-(4-nitrophenyl)-imidazo[4,5-*f*][1,10]phenanthroline (PNOPH), 2-(3-nitrophenyl)imidazo[4,5-*f*][1,10]phenanthroline (MNOPH) and 2-(2-nitrophenyl)imidazo[4,5-*f*][1,10]phenanthroline (ONOPH)] and their deprotonated complexes have been synthesized and characterized. The electrochemical behaviour of these complexes were examined and compared to that of $[Ru(dmb)_3]^{2+}$. Non-linear optical (NLO) properties of the complexes were investigated using Z-scan techniques. All of the complexes exhibit both NLO absorption and self-defocusing effect ($n_2 = -0.79 \times 10^{-17}$ to -1.44×10^{-17} m^2 W^{-1}, $\alpha_2 = 3.00 \times 10^{-11}$ to 7.09×10^{-11} m W^{-1}, [M] = 5×10^{-5} mol dm^{-3} in acetonitrile solution). The corresponding effective NLO susceptibilities $|\chi^{(3)}|$ of the complexes are 2.86×10^{-12} to 5.07×10^{-12} esu. The results indicate that the substitution and deprotonation of the ligand have an effect on the NLO properties of the complexes. Finally, the crystal structure of $[Ru(dmb)_2(PNOP)][ClO_4]\cdot H_2O\cdot 0.5C_6H_6$ was determined by X-ray diffraction analysis; it contains two twisted dmb ligands and the bidentate ligand PNOP with torsional angles between each dmb ring pair of 3.4 and 8.7°.

Tremendous interest has been attracted to non-linear optical (NLO) processes because of their potential in photonic applications.[1,2] However, this activity has primarily focused on purely organic systems[1,2] and, to a far lesser extent, on organometallic and coordination complexes.[3] Compared to organic molecules, metal complexes can have a larger variety of structures with comparable or, in some cases, higher environmental stability and a much greater diversity of tunable electronic properties by virtue of the coordinate metal centre.

Recently, ruthenium complexes have received considerable attention as NLO materials due to their rich photochemical properties and varied coordination forms.[4] Several notable reports show that mixed-valence,[5] 2,2′-bipyridine (bpy),[6] and σ-acetylide complexes[7] can exhibit extremely large β values. Other types of ruthenium complexes with high β values are also being studied.[8] In contrast, although the third-order NLO properties of this kind of compound have received a limited degree of attention,[9–11] their vast potential as third-order NLO materials remains largely untapped.

The phenanthroimidazolebenzene derivatives are candidates for third-order NLO materials by virtue of their high third harmonic generation and rapid response.[12] Their analogues, 2-phenylimidazo[4,5-*f*][1,10]phenanthroline and its derivatives, have recently been synthesized.[13,14] Since these compounds possess phenanthrolinyl groups, they are potential ligands for metals such as ruthenium. We present here three new ruthenium(II) complexes with $[Ru(dmb)_2]^{2+}$ centres, together with their deprotonated complexes (Chart 1). The third-order NLO properties of the complexes were measured by Z-scan techniques.[15–17] Unlike second-order NLO materials, the structure–property relationships that govern third-order NLO polarization are a little vague. This study provides an opportunity to assess the effects of deprotonation and substitution of the ligand on the third-order NLO properties of the ruthenium(II) complexes.

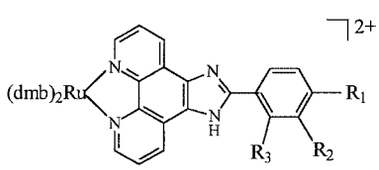

PNOPH: $R_1 = NO_2$, $R_2 = R_3 = H$,
MNOPH: $R_2 = NO_2$, $R_1 = R_3 = H$,
ONOPH: $R_3 = NO_2$, $R_1 = R_2 = H$.

Chart 1 Structures of the ruthenium(II) complexes.

Experimental

Syntheses

The compounds *cis*-$[Ru(dmb)_2Cl_2]\cdot 2H_2O$ (dmb = 4,4′-dimethyl-2,2′-bipyridine),[18] 2-(2-nitrophenyl)imidazo[4,5-*f*][1,10]phenanthroline (ONOPH),[13] 2-(3-nitrophenyl)imidazo[4,5-*f*][1,10]phenanthroline (MNOPH)[13] and 2-(4-nitrophenyl)-imidazo[4,5-*f*][1,10]phenanthroline (PNOPH)[14] were prepared

† *Supplementary data available*: rotatable 3-D crystal structure diagram in CHIME format. See http:/www.rsc.org/suppdata/dt/1999/3711/

according to the literature procedures. Other materials were commercially available and of reagent grade.

[Ru(dmb)$_2$(PNOPH)][ClO$_4$]$_2$·2H$_2$O 1. A mixture of *cis*-[Ru(dmb)$_2$Cl$_2$]·2H$_2$O (0.5 mmol, 0.288 g), ONOPH (0.5 mmol, 0.171 g) and ethanol (30 cm^3) was refluxed under argon for 5 h during which time the solution colour changed from purple to red. The ethanol was evaporated to dryness, the solid was taken up in H_2O, and the mixture was filtered to remove unreacted ligand, a red precipitate was obtained by dropwise addition of a saturated aqueous $NaClO_4$ solution. The product was purified by column chromatography on alumina using acetonitrile–toluene (2:1 v/v) as eluent and then dried *in vacuo*. Yield 0.334 g, 63.9% (Found: C, 49.6; H, 3.6; N, 12.4. Calc. for $C_{43}H_{39}Cl_2N_9O_{12}Ru$: C, 49.4; H, 3.7; N, 12.1%). ν_{max}/cm^{-1} 3417 (N–H), 3070 (C–H), 1616 (C=N), 1532 (NO_2) and 1092 (ClO_4^-). MS [ESMS (CH_3OH), *m*/*z*] 810 ([M − 2ClO$_4$]$^+$), 405.7 ([M − 2ClO$_4$]$^{2+}$). ^{1}H NMR [(CD$_3$)$_2$SO]: δ 9.11 (d, 2H), 8.72 (s, 2H), 8.68 (s, 2H), 8.62 (d, 2H), 8.46 (d, 2H), 8.02 (d, 2H), 7.89 (dd, 2H), 7.66 (d, 2H), 7.40 (m, 4H), 7.16 (d, 2H), 2.56 (s, 6H) and 2.48 (s, 6H).

[Ru(dmb)$_2$(MNOPH)][ClO$_4$]$_2$·H$_2$O 2. This complex (deep red) was synthesized in a similar manner to that described for [Ru(dmb)$_2$(PNOPH)][ClO$_4$]$_2$·2H$_2$O, with 0.5 mmol, 0.171 g MNOPH in place of PNOPH. Yield 0.288 g, 56% (Found: C, 50.4; H, 3.5; N, 12.4. Calc. for $C_{43}H_{37}Cl_2N_9O_{11}Ru$: C, 50.2; H, 3.6; N, 12.3%). ν_{max}/cm^{-1} 3423 (N–H), 3071 (C–H), 1616 (C=N), 1532 (NO_2) and 1089 (ClO_4^-). MS [ESMS (CH_3OH), *m*/*z*] 810 ([M − 2ClO$_4$]$^+$), 405.7 ([M − 2ClO$_4$]$^{2+}$). ^{1}H NMR [(CD$_3$)$_2$SO]: δ 9.15 (s, 1H), 9.10 (d, 2H), 8.79 (d, 1H), 8.72 (s, 2H), 8.68 (s, 2H), 8.37 (d, 1H), 8.03 (d, 2H), 7.91 (m, 3H), 7.66 (d, 2H), 7.38 (m, 4H), 7.16 (d, 2H), 2.56 (s, 6H) and 2.48 (s, 6H).

[Ru(dmb)$_2$(ONOPH)][ClO$_4$]$_2$·H$_2$O 3. This complex (deep red) was synthesized in a similar manner to that described for [Ru(dmb)$_2$(PNOPH)][ClO$_4$]$_2$·2H$_2$O, with 0.5 mmol, 0.171 g ONOPH in place of PNOPH. Yield 0.313 g, 61% (Found: C, 50.3; H, 3.8; N, 12.3. Calc. for $C_{43}H_{37}Cl_2N_9O_{11}Ru$: C, 50.2; H, 3.6; N, 12.3%). ν_{max}/cm^{-1} 3420 (N–H), 3071 (C–H), 1616 (C=N), 1532 (NO_2) and 1089 (ClO_4^-). MS [ESMS (CH_3OH), *m*/*z*] 810 ([M − 2ClO$_4$]$^+$), 405.7 ([M − 2ClO$_4$]$^{2+}$). ^{1}H NMR [(CD$_3$)$_2$SO]: δ 8.95 (d, 2H), 8.72 (s, 2H), 8.68 (s, 2H), 8.17 (dd, 2H), 8.08 (d, 2H), 7.98 (t, 2H), 7.88 (m, 2H), 7.66 (d, 2H), 7.41 (d, 4H), 7.15 (d, 2H), 2.56 (s, 6H) and 2.48 (s, 6H).

[Ru(dmb)$_2$(PNOP)][ClO$_4$]·H$_2$O 4. A solution of complex **1** (0.144 mmol, 0.15 g) in methanol was added to a sodium methoxide solution which was made *in situ* by dissolving sodium metal (0.72 mmol, 0.017 g) in methanol (10 cm^3). The colour of the solution changed from red to dark red. The solution was heated while stirring for 30 min and then cooled to 0–5 °C in a refrigerator. A deep red microcrystalline solid was collected by filtration. Yield 0.096 g, 72% (Found: C, 55.7; H, 3.8; N, 13.3. Calc. for $C_{43}H_{36}ClN_9O_7Ru$: C, 55.7; H, 3.9; N, 13.6%). ^{1}H NMR [(CD$_3$)$_2$SO]: δ 8.92 (d, 2H), 8.72 (s, 2H), 8.68 (s, 2H), 8.59 (d, 2H), 8.28 (d, 2H), 7.78 (d, 2H), 7.70 (m, 4H), 7.39 (t, 4H), 7.18 (d, 2H), 7.15 (d, 2H), 2.55 (s, 6H) and 2.45 (s, 6H). Crystals suitable for an X-ray crystallographic study were grown from acetonitrile–benzene (1:1, v/v) at room temperature.

[Ru(dmb)$_2$(MNOP)][ClO$_4$]·H$_2$O 5. The complex was synthesized in a similar manner to that described for complex **4**, using complex **2** in place of complex **1**. Yield 0.104 g, 78% (Found: C, 55.9; H, 3.9; N, 13.8. Calc. for $C_{43}H_{36}ClN_9O_7Ru$: C, 55.7; H, 3.9; N, 13.6%). ^{1}H NMR [(CD$_3$)$_2$SO]: δ 9.14 (s, 1H), 8.96 (d, 2H), 8.77 (d, 1H), 8.73 (s, 2H), 8.69 (s, 2H), 8.30 (s, 1H), 8.10 (d, 1H), 7.78 (d, 2H), 7.70 (m, 4H), 7.40 (d, 2H), 7.37 (d, 2H), 7.17 (d, 2H) and 2.49 (m, 12H).

[Ru(dmb)$_2$(ONOP)][ClO$_4$]·3H$_2$O 6. The complex was synthesized in a similar manner to that described for complex **4**, using complex **3** in place of complex **1**. Yield 0.09 g, 65% (Found: C, 53.8; H, 4.0; N, 13.2. Calc. for $C_{43}H_{40}ClN_9O_9Ru$: C, 53.6; H, 4.2; N, 13.1%). ^{1}H NMR [(CD$_3$)$_2$SO]: δ 8.81 (d, 2H), 8.72 (s, 2H), 8.67 (s, 2H), 8.29 (d, 1H), 7.78 (d, 2H), 7.69 (m, 5H), 7.49 (m, 1H), 7.40 (d, 2H), 7.37 (d, 1H), 7.25 (t, 1H), 7.17 (d, 1H), 7.14 (s, 2H) and 2.49 (m, 12H). **CAUTION:** perchlorate salts of metal complexes with organic ligands are potentially explosive, and only small amounts of the material should be prepared and handled with great care.

Physical measurements

The analyses (C, H and N) were performed using a Perkin-Elmer 240Q elemental analyser. Infrared spectra were obtained with a Nicolet 170SX-FTIR spectrophotometer and KBr discs, UV/VIS spectra on a Shimadzu MPS-2000 spectrophotometer and ^{1}H NMR spectra on a Varian 500 MHz spectrometer with (CD$_3$)$_2$SO as solvent at room temperature and $SiMe_4$ as an internal standard. Electrospray mass spectra (ES-MS) were recorded on a LCQ system (Finnigan MAT, USA) using methanol as mobile phase. The spray voltage, tube lens offset, capillary voltage and capillary temperature were set at 4.50 kV, 30.00 V, 23.00 V and 200 °C, respectively, and the quoted *m*/*z* values are for the major peaks in the isotope distribution.

Cyclic voltammetry was performed on an EG & G PAR 273 polarographic analyser and 270 universal programmer. The supporting electrolyte was 0.1 mol dm^{-3} tetrabutylammonium perchlorate in acetonitrile freshly distilled from phosphorus pentoxide and deaerated by purging with nitrogen. A standard three-electrode system was used comprising a platinum microcylinder working electrode, platinum-wire auxiliary electrode and a saturated calomel reference electrode (SCE).

Crystallography

Crystal data and data collection parameters. $C_{46}H_{34}ClN_9O_7Ru$ (**4**·0.5C_6H_6), M = 961.34, triclinic, space group $P\bar{1}$, a = 9.0170(5), b = 11.4957(6), c = 22.1396(12) Å, U = 2232.3(2) Å^3, Z = 2, λ(Mo-Kα) = 0.71073 Å, μ = 0.472 mm^{-1}, T = 293(2) K, deep red prism with dimensions 0.50 × 0.30 × 0.20 mm. Bruker SMART 1000 CCD diffractometer, ω scans, data collection range $1.80 < \theta < 23.30°$, $-7 \le h \le 10$, $-12 \le k \le 10$, $-24 \le l \le 24$, 9962 reflections measured, 6407 unique (R_{int} = 0.0176) which were used in all calculations.

Structure solution and refinement. The structure was solved by direct methods using SHELXS-97[36] and refined anisotropically on F^2 by full-matrix least-squares techniques. All hydrogen atoms were generated geometrically (C–H 0.96 Å). Refinement of 577 parameters converged at R_1 [for selected data with $I > 2\sigma(I)$] = 0.0475, wR_2 (for all data) = 0.1399. The largest residual peak and hole were +1.025 and −0.662 e Å^{-3}.

CCDC reference number 186/1645.

See http://www.rsc.org/suppdata/dt/1999/3711/ for crystallographic files in .cif format.

Non-linear optical measurements

Acetonitrile solutions of 5.0 × 10^{-5} mol dm^{-3} of the ruthenium(II) complexes were placed in a 2 mm quartz cuvette for optical measurements. Their non-linear refraction and non-linear absorption were measured with a linearly polarized laser light (λ = 540 nm; pulse width (FWHM) = 12 ns) generated from an excimer laser (Lambda Physics EMG 201MSC)–pumped dye laser (Lambda Physics model FL2002) system. The spatial profiles of the optical pulses were nearly Gaussian. The laser beam was focused with a 4.5 cm focal length focusing mirror. The radius of the beam waist at the focus point was measured to be 30 μm (half width at 1/e^2 maximum). The

repetition rate of the laser pulse was 10 Hz. The incident and transmitted pulse energy were measured by a Laser Precision detector (RJ-7200 energy probe). The NLO properties of the samples were manifested by moving the samples along the axis of incident beam (*z* direction) with respect to the focal point. An aperture of 0.5 mm radius was placed in front of the detector to assist the measurement of the self-defocusing effect. The set-up for the optical measurements is shown in Fig. 1.

Results and discussion

Syntheses

The reaction of $[Ru(dmb)_2Cl_2]\cdot 2H_2O$ with the appropriate ligands in ethanol gave the desired mixed-ligand complexes as perchlorates. These new complexes are soluble in acetone and acetonitrile, and relatively soluble in ethanol and methanol. To obtain pure complexes, the products were purified by column chromatography and characterized by electrospray MS and elemental analyses. Deprotonation was achieved by reaction of sodium methoxide with the ruthenium(II) complexes in methanol. The structure of the deprotonated complex $[Ru(dmb)_2(PNOP)][ClO_4]$ was further confirmed by single crystal X-ray structure analysis described below. The deprotonated complexes completely reverted to the corresponding protonated ones on the addition of acid.

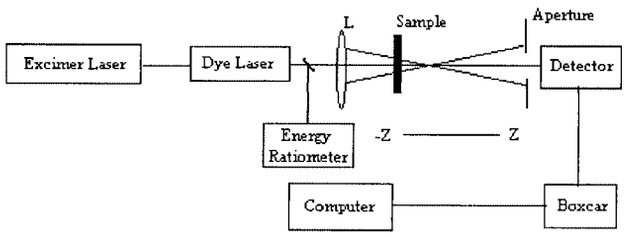

Fig. 1 Schematic illustration of the experimental set-up for Z-scan measurements.

^{1}H NMR spectra

All of the new ruthenium(II) complexes give well-defined ^{1}H NMR spectra, which permit unambiguous identification and assessment of purity. The deprotonation of LH (LH = PNOPH, MNOPH or ONOPH) in the ruthenium(II) complex induces an upfield shift for all proton signals in L (for example, see Fig. 2). Shifts in the dmb resonances are small but nevertheless significant. The shift in the resonance positions of the protons in L can be explained by the increased electron density in the imidazole ring,[19] which probably also delocalizes the electron density in the whole π framework of the ligand L. Also the change in the overall charge of the compound is likely to influence the resonance frequencies.[19]

Crystal structure of $[Ru(dmb)_2(PNOP)][ClO_4]\cdot H_2O\cdot 0.5C_6H_6$

The molecular structure of $[Ru(dmb)_2(PNOP)][ClO_4]\cdot H_2O\cdot 0.5C_6H_6$ (**4**·$0.5C_6H_6$) has been confirmed by single-crystal X-ray diffraction analysis. It consists of a $[Ru(dmb)_2(PNOP)]^+$ cation, a disordered ClO_4^- anion, a lattice water and half a benzene solvent molecule in an asymmetric region. An ORTEP[20] view of the cation is illustrated in Fig. 3. Selected bond lengths and angles are given in Table 1.

As shown in Fig. 3, the central ruthenium atom is chelated by two dmb ligands oriented in a *cis* geometry and a PNOP ligand. The co-ordination geometry around the ruthenium atom is that of a distorted octahedron, with a bite angle of 78.68° averaged over the three bidentate ligands. This distortion from

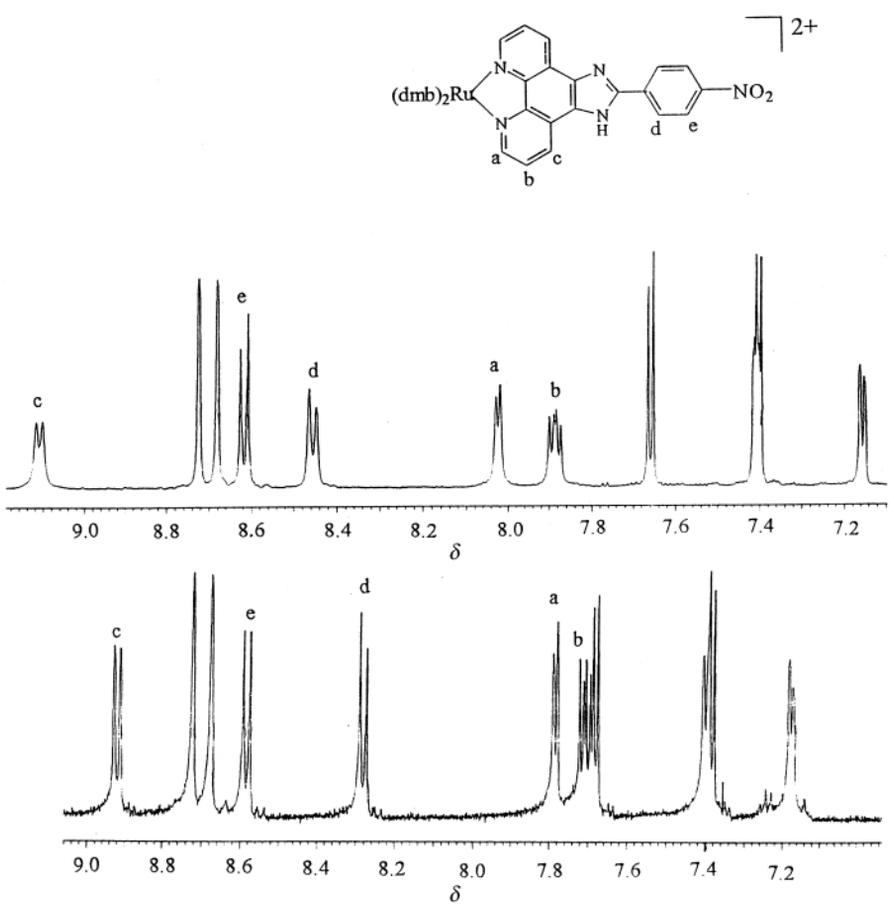

Fig. 2 The ^{1}H NMR spectra of $[Ru(dmb)_2(PNOPH)]^{2+}$ (top) and $[Ru(dmb)_2(PNOP)]^+$ (bottom) in the aromatic region between $\delta = 7.0$ and $\delta = 9.2$ [$(CD_3)_2SO$ solvent; TMS reference].

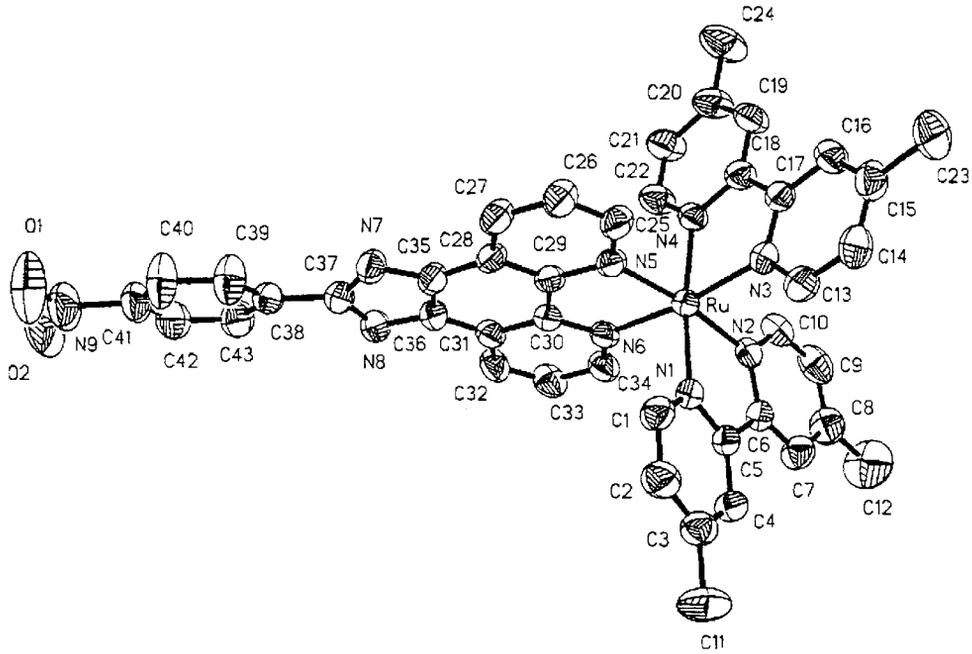

Fig. 3 An ORTEP drawing of $[Ru(dmb)(PNOP)]^{+}$ and the atom numbering.

Table 1 Selected bond lengths (Å) and angles (°) for $[Ru(dmb)_2(PNOP)][ClO_4]\cdot H_2O\cdot 0.5C_6H_6$

Ru–N(1)	2.060(4)	Ru–N(4)	2.057(4)
Ru–N(2)	2.059(4)	Ru–N(5)	2.058(4)
Ru–N(3)	2.062(4)	Ru–N(6)	2.061(4)
N(4)–Ru–N(2)	97.15(14)	N(3)–Ru–N(6)	172.52(13)
N(4)–Ru–N(5)	88.92(14)	C(1)–N(1)–Ru	126.6(3)
N(2)–Ru–N(5)	172.33(13)	C(5)–N(1)–Ru	116.3(3)
N(4)–Ru–N(1)	173.41(13)	C(10)–N(2)–Ru	126.7(3)
N(2)–Ru–N(1)	78.23(14)	C(6)–N(2)–Ru	116.2(3)
N(5)–Ru–N(1)	96.09(14)	C(17)–N(3)–Ru	116.4(3)
N(4)–Ru–N(3)	78.41(14)	C(13)–N(3)–Ru	126.2(3)
N(2)–Ru–N(3)	90.73(14)	C(22)–N(4)–Ru	126.8(3)
N(5)–Ru–N(3)	95.09(14)	C(18)–N(4)–Ru	115.7(3)
N(1)–Ru–N(3)	96.84(14)	C(25)–N(5)–Ru	128.4(3)
N(4)–Ru–N(6)	96.32(14)	C(29)–N(5)–Ru	114.3(3)
N(2)–Ru–N(6)	95.22(13)	C(34)–N(6)–Ru	127.7(3)
N(5)–Ru–N(6)	79.39(13)	C(30)–N(6)–Ru	114.5(3)
N(1)–Ru–N(6)	88.82(14)		

an ideal octahedral geometry (90°) can be rationalized by the restrictions imposed by the ligands. The torsion angles between the 4-methylpyridine pairs of two dmb ligands of the complex are non-equivalent, one being 3.4° and the other 8.7°; however, they are all located in the range expected for this type of compound such as $[Ru(bpy)_2(gly)]^{+}$ (gly = glycinate) (1.4 and 7.4°),[21] $[Ru(bpy)_2(ip)]^{2+}$ (ip = imidazo[4,5-*f*][1,10]phenanthroline) (5.7 and 8.6°),[22] $[Ru(bpy)_2(phen)]^{2+}$ (6.4 and 10.3°)[23] and $[Ru(bpy)_2(mphen)]^{2+}$ (mphen = 5-methyl-1,10-phenanthroline) (1.9 and 12.3°).[23]

The mean Ru–N bond length (2.0595 Å) is comparable with those published for $[Ru(bpy)_3]^{2+}$ (2.056 Å),[24] $[Ru(bpy)_2(phen)]^{2+}$ (2.069 Å)[23] and $[Ru(phen)_3]^{2+}$ (2.063 Å),[25] although there are larger differences in size and shape for bpy, dmb, phen and PNOP. There are two ways of explaining why these Ru–N bond lengths are similar to each other. One may be that the changes in σ bonding are almost balanced by those in π bonding of the Ru–N with change of ligand structure such that the interatomic Ru–N are basically constant.[24] Another possible interpretation is that these bonds are not particularly sensitive to the total electronic density, as seen in the structures of $[Ru(bpy)_3]$, $[Ru(bpy)_3]^{2+}$ and $[Ru(bpy)_3]^{3+}$.[26]

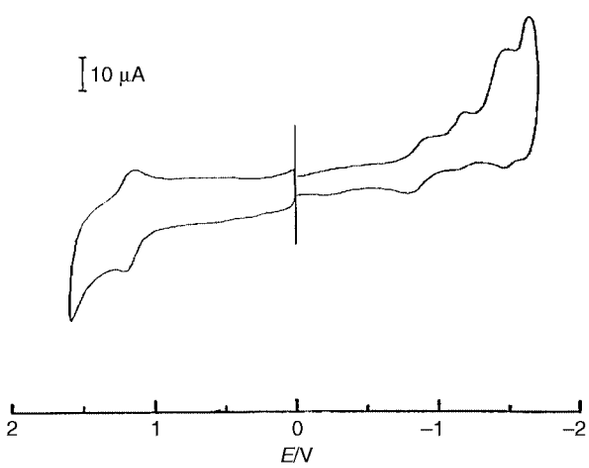

Fig. 4 Cyclic voltammogram of $[Ru(dmb)(PNOPH)]^{2+}$.

Table 2 Redox potentials for the ruthenium(II) complexes[a]

	$E_{1/2}$/V (ΔE_p[b]/mV)			
Complex	Oxidations		Reductions	
1	1.20(60)	−0.88(75)	−1.17(63)	−1.52(63)
2	1.20(65)	−0.89(100)	−1.20(75)	−1.53(75)
3	1.20(65)	−0.85(100)	−1.25(75)	−1.51(87)
4	1.17(60)	−0.83(72)	−1.14(75)	−1.51(75)
5	1.17(60)	−0.85(63)	−1.18(75)	−1.52(100)
6	1.17(60)	−0.82(65)	−1.22(73)	−1.50(100)

[a] All complexes were measured in 0.1 M NBu_4ClO_4–CH_3CN, error in potentials was ±0.02 V; $T = 23 \pm 1$ °C; scan rate = 100 mV s^{-1}; ΔE_p in parentheses. [b] $\Delta E_p = E_{1/2}(ox) - E_{1/2}(red)$.

Electrochemistry

The electrochemical behaviour of the complexes has been studied in CH_3CN by cyclic volammetry. Results are collected in Table 2. Each complex exhibits well shaped oxidation (one) and reduction (three) waves in the sweep range from −1.8 to +1.6 V, as shown in Fig. 4 for $[Ru(dmb)_2(PNOPH)]^{2+}$. This pattern is common to most d^6 metal polypyridyl

Table 3 Absorption spectral data of ligands and complexes

Compound	λ_{max}/nm (ε/M^{-1} cm^{-1})
PNOPH [a,c]	372w (7850), 256(sh) (11710), 228 (7520)
MNOPH [a,d]	320.9 (33100), 303.5(sh) (32650), 270.7 (55350), 242.5 (31750), 213.5 (34250)
ONOPH [a,d]	357(sh) (5940), 281.1(sh) (47800), 240.1 (57950), 213.5 (4535)
$Ru(dmb)_2(PNOPH)^{2+}$ [b]	463 (15780), 349 (24420), 284 (64120), 259 (33760), 248 (34780)
$Ru(dmb)_2(MNOPH)^{2+}$ [b]	463 (10320), 283 (58920), 259 (26900), 248 (28600)
$Ru(dmb)_2(ONOPH)^{2+}$ [b]	460 (12586), 284 (64020), 259 (30480), 248 (31160)
$Ru(dmb)_2(PNOP)^{+}$ [b]	468(sh), 455 (17580), 384 (21360), 286 (52200), 259 (25180), 247 (25500)
$Ru(dmb)_2(MNOP)^{+}$ [b]	466 (10060), 328 (21540), 289 (53080), 258 (19700), 248 (20720)
$Ru(dmb)_2(ONOP)^{+}$ [b]	464 (10540), 318 (17440), 286 (51580), 259 (21800), 248 (21260)

[a] In ethanol. [b] In CH_3CN. [c] Ref. 14. [d] Ref. 13.

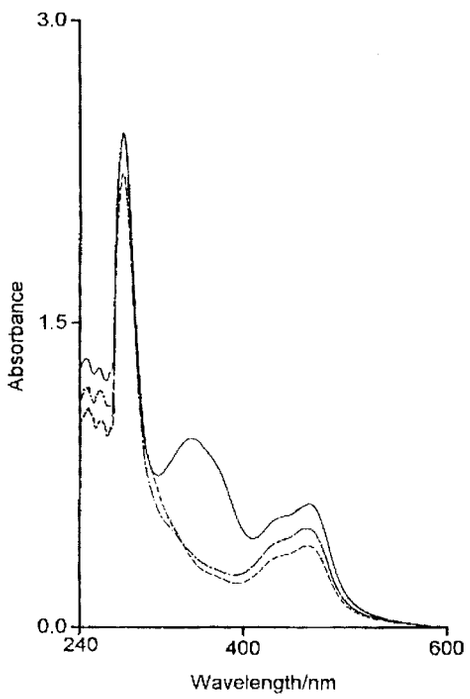

Fig. 5 The UV/VIS spectra of complex **1** (full line), **2** (broken line) and **3** (dot-dash line) in acetonitrile.

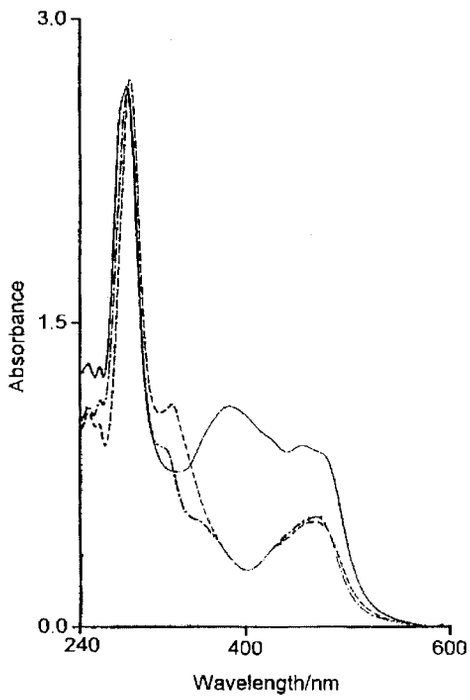

Fig. 6 The UV/VIS spectra of complex **4** (full line), **5** (broken line) and **6** (dot-dash line) in acetonitrile.

complexes where the redox orbitals are localized on the individual ligands.[27] The anodic and cathodic peak separations vary from 60 to 100 mV and are almost scan rate independent, indicating that the processes are reversible one-electron transfers.

Oxidation of the complexes involves removal of an electron from the d_π orbital of Ru^{II}, while reduction involves transfer of an electron to the ligand-centred orbitals. The locations of the NO_2 group in the ligand have a negligible effect on the redox potentials of the complexes. Upon deprotonation of the complexes of **1**, **2** and **3**, the oxidation potential shifts to slightly more negative potential. This suggests that the electron density on the Ru ion increases as a result of the strong σ-donor property of deprotonated ligands. For all of the complexes the first two reductions are obviously assigned to the ligand (PNOPH, MNOPH or ONOPH), and the last reduction is characteristic of the two dmb ligands.[28]

Absorption spectra

The spectral data for the complexes are collected in Table 3. Absorption spectra of the complexes **1**, **2** and **3** were obtained in CH_3CN (Fig. 5). The spectra of the three complexes consist of three well resolved bands in the range of 200 to 700 nm except complex **1**, in which a band at 349 nm is observed besides the three bands. The bands at 284, 259 and 248 nm are attributed to intraligand π–π* transitions by comparison with the spectrum of $[Ru(dmb)_3]^{2+}$.[18] The band at 349 nm of complex **1** is attributed to the π–π* (PNOPH) transition in comparison with the absorption spectrum of the free ligand PNOPH. The lowest energy bands at 463, 463 and 461 nm for complexes of **1**, **2** and **3** are assigned to the metal–ligand charge transfer (MLCT) transitions. These bands are bathochromically shifted by comparison with that of $[Ru(dmb)_3]^{2+}$,[18] which can be attributed to the extension of the corresponding π framework.

Absorption spectra of three deprotonated complexes of **4**, **5** and **6** were also obtained in CH_3CN (Fig. 6). There are some changes in comparison with those of complexes of **1**, **2** and **3**. For complex **4** the π–π* (L) transition is red shifted to 384 nm, the π–π* (L) transition is also observed at 328 nm for complex **5** and 318 nm for complex **6**. This suggests that the deprotonated ligands have a larger extent of π delocalization. At the same time, the MLCT bands of the deprotonated complexes all red shift. The slight lowering in the MLCT energies indicates that the deprotonated ligand is a stronger σ-donor ligand.

Non-linear optical properties

All the six ruthenium(II) complexes exhibit both non-linear optical refraction and non-linear optical absorption. The non-linear absorption component was evaluated under an open

Table 4 Measurement results of the Ru^{II} complexes using Z-scan techniques

Complex	ΔT_{v-p}	I_0/W m^{-2}	α/cm^{-1}	n_2/m^2 W^{-1}	α_2/m W^{-1}	$\chi^{(3)}$/esu[a]	γ/esu[a]
1	0.144	1.21×10^{12}	1.39	-1.44×10^{-17}	7.09×10^{-11}	5.07×10^{-12}	6.46×10^{-29}
2	0.130	1.72×10^{12}	1.20	-0.90×10^{-17}	3.00×10^{-11}	3.13×10^{-12}	3.99×10^{-29}
3	0.157	1.74×10^{12}	1.80	-1.14×10^{-17}	4.98×10^{-11}	3.99×10^{-12}	5.09×10^{-29}
4	0.179	2.07×10^{12}	1.70	-1.08×10^{-17}	5.77×10^{-11}	3.82×10^{-12}	4.87×10^{-29}
5	0.129	2.05×10^{12}	1.80	-0.79×10^{-17}	5.97×10^{-11}	2.86×10^{-12}	3.65×10^{-29}
6	0.183	2.05×10^{12}	1.20	-1.06×10^{-17}	5.55×10^{-11}	3.74×10^{-12}	4.77×10^{-29}

[a] Values ± 10%.

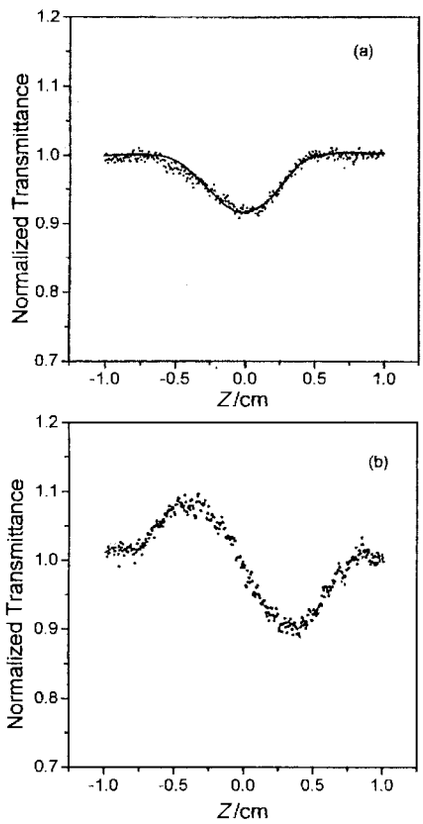

Fig. 7 Z-scan data (filled circles) of 5×10^{-5} mol dm^{-3} of $[Ru(dmb)_2(ONOP)][ClO_4]\cdot 3H_2O$, at 540 nm with $I(Z = 0)$ being 2.05×10^{12} W m^{-2}: (a) collected under open aperture configuration showing NLO absorption. The solid curve is a theoretical fit based on eqns. (1) and (2); (b) obtained by dividing the normalized Z-scan data obtained under closed aperture configuration by the normalized Z-scan data in (a). It shows the self-defocusing effect of the complex.

aperture configuration, for example see Fig. 7a. Light transmittance (T) is a function of incident light irradiance $I_i(Z)$, non-linear absorption ($\alpha_2 = \alpha_2(I_i)$), and linear absorption (α_0) as illustrated in eqns. (1) and (2).[15,16]

$$T(Z) = \frac{1}{q(z)\sqrt{\pi}} \int_{-\infty}^{+\infty} \ln[1 + q(Z)]\exp(-\tau^2)\, d\tau \qquad (1)$$

$$q(Z) = \alpha_2 I_i(Z) \frac{(1 - e^{-\alpha_0 L})}{\alpha_0} \qquad (2)$$

The α_2 value can in turn be determined by fitting a theoretical curve, $T(Z)$, to the Z-scan data according to eqns. (1) and (2). The solid line in Fig. 7a is a theoretical curve that fits best to the Z-scan data observed under the open aperture configuration.

The non-linear refractive property of the ruthenium(II) complexes was assessed by dividing the normalized Z-scan data obtained under closed aperture configuration by the normalized Z-scan data obtained under open aperture configuration, for example see Fig. 7b. This procedure helps to extract information of NLO refraction from a raw data set containing mixed information on both refraction and absorption.[16,17] The valley/peak pattern of the corrected transmittance curve so obtained shows the characteristic self-defocusing behaviour of propagating light in the sample.

The difference between normalized transmittance values at valley and peak portions, ΔT_{v-p} can be related to the non-linear refractive index n_2 (m^2 W^{-1}) by eqn. (3), where n_2 is defined by

$$n_2 = \frac{\lambda a_0}{0.812\pi I(1 - e^{-\alpha_0 L})} \Delta T_{v-p} \qquad (3)$$

$n = n_0 + n_2 I$. With measured values of ΔT_{v-p}, a_0 and L, the n_2 value can be calculated. The values of α_2 and n_2 are listed in Table 4.

In accordance with the α_2 and n_2 values, the modulus of the effective third-order susceptibility $\chi^{(3)}$ can be calculated [eqn. (4)][29] where λ is the wavelength of the laser (λ = 540 nm).

$$|\chi^{(3)}| = \sqrt{\left|\frac{c\lambda n_0^2}{64\pi^3}\alpha_2\right|^2 + \left|\frac{cn_0^2}{16\pi^2}n_2\right|^2} \qquad (4)$$

The corresponding modulus of the hyperpolarizability γ can be obtained from $|\chi^{(3)}| = N\left(\frac{n_0^2 + 2}{3}\right)^4 |\gamma|$, where N is the number density of the solute in the solution (in cm^{-3}), and n_0 is the linear index of refraction of the complexes. The values of $|\chi^{(3)}|$ and $|\gamma|$ are also listed in Table 4.

It should be emphasized that the Z scans reported here could not reveal the origins of the observed non-linearities. Both excited state absorption and two-photon absorption can be responsible for the measured NLO effects. The existing experimental data are insufficient to allow identification of the relative contributions of these two mechanisms. The NLO parameters derived in this paper should be regarded as effective parameters only. The $|\gamma|$ values obtained for the new complexes are large, and comparable with those of some known NLO chromophores (1.6×10^{-28} esu for a half-open cubane-like $[WOS_3(CuBr)_3(\mu\text{-}Br)]^{3-}$ at 532 nm,[30] 9×10^{-29} esu for a butterfly-shaped $[WOS_3Cu_2(PPh_3)_4]$ at 532 nm,[31] 5.6×10^{-35} to 8.6×10^{-34} esu for Group 10 metal alkynyl polymers at 1064 nm,[32,33] 9.3×10^{-35} to 3.6×10^{-33} esu for some octopolar alkynylruthenium complexes at 800 nm,[11] 1×10^{-32} to 1×10^{-31} esu for metallophthalocyanines at 1064 nm[34] and 7.5×10^{-34} esu for C_{60} at 1910 nm[35]). The data (**1** *cf.* **2** *cf.* **3**) suggest that the sites of the substituent group in the ligand exert an influence on the NLO properties of the complexes and the values of $|\gamma|$ increase in the order: MNOPH < ONOPH < PNOPH. Inspection of $|\gamma|$ (**1** *cf.* **4**; **2** *cf.* **5**; **3** *cf.* **6**) reveals a slight decrease in this parameter upon deprotonation though the difference between complex **2** and complex **5** (or complex **3** and complex **6**) is negligible considering the experimental errors in the data. This can be attributed to the decreased π-acceptor capacity of the ligand, resulting in decreasing π back-donation of the metal and blocking the extension of the electronic π-system.

Acknowledgements

We are grateful to the National Natural Science foundation of China, Natural Science foundation of Guangdong Province and the State Key Laboratory of Coordination Chemistry at Nanjing University for their financial support.

References

1 *Molecular Nonlinear Optics*, ed. J. Zyss, Academic Press, New York, 1994; *Materials for Nonlinear Optics: Chemical Perspectives*, eds. S. R. Marder, J. E. Sohn and G. D. Stucky, ACS Symposium Series 455, American Chemical Society, Washington, DC, 1991; *Organic Molecules for Nonlinear Optics and Photonics*, eds. J. Messier, F. Kajzar and P. Prasad, Kluwer Academic Publishers, Dordrecht, 1991.
2 For recent reviews on NLO materials see for example: L. R. Dalton, A. W. Harper, R. Ghosn, W. H. Steir, M. Ziari, H. Fetterman, Y. Shi, R. V. Mustacich, A. K. Y. Jen and K. J. Shea, *Chem. Mater.*, 1995, **7**, 1060; R. G. Benning, *J. Mater. Chem.*, 1995, **5**, 365; T. J. Marks and M. A. Ratner, *Angew. Chem.*, *Int. Ed. Engl.*, 1995, **34**, 155; *Optical Nonlinearities in Chemistry*, eds. D. M. Burland, *Chem. Rev.*, 1994, **94**, 1.
3 S. R. Marder, in *Inorganic Materials*, eds. D. W. Bruce and D. O'Hare, Wiley, Chichester, 1992; N. J. Long, *Angew. Chem.*, *Int. Ed. Engl.*, 1995, **34**, 21; H. S. Nalwa, *Appl. Organomet. Chem.*, 1991, **5**, 349.
4 M. Schroder and T. A. Stephenson, in *Comprehensive Coordination Chemistry*, eds. G. Wilkinson, R. D. Gillard and J. A. McCleverty, Pergamon, Oxford, 1987, vol. 4.
5 W. M. Laidlaw, R. G. Denning, T. Verbiest, E. Chauchard and A. Persoons, *Nature* (*London*), 1993, **363**, 58; *Proc. SPIE. Int. Soc. Opt. Eng.*, 1994, **2143**, 14.
6 C. Dhenaut, I. Ledoux, I. D. W. Samuel, J. Zyss, M. Bourgault and H. Le Bozec, *Nature* (*London*), 1995, **374**, 339.
7 I. R. Whittall, M. G. Humphrey, A. Persoons and S. Houbrechts, *Organometallics*, 1996, **15**, 1935; S. Houbrechts, K. Clays, A. Persoons, V. Cadierno, M. P. Gamasa and J. Gimeno, *Organometallics*, 1996, **15**, 5266.
8 B. J. Coe, G. Chadwick, S. Houbrechts and A. Persoons, *J. Chem. Soc.*, *Dalton Trans.*, 1997, 1705; B. J. Coe, J. P. Essex-Lopresti, J. A. Harris, S. Houbrechts and A. Persoons, *Chem. Commun.*, 1997, 1645; B. J. Coe, M. C. Chamberlain, J. P. Essex-Lopresti, S. Gaines, J. C. Jeffery, S. Houbrechts and A. Persoons, *Inorg. Chem.*, 1997, **36**, 3284; B. J. Coe, J. A. Harris, L. J. Harrington, J. C. Jeffery, L. H. Rees, S. Houbrechts and A. Persoons, *Inorg. Chem.*, 1998, **37**, 3391; B. J. Coe, S. Houbrechts, I. Asselberghs and A. Persoons, *Angew. Chem.*, *Int. Ed.*, 1999, **38**, 366.
9 A. R. Dias, M.-H. Garcia, J. C. Rodrignes, J. C. Petersen, T. Bjoemholm and T. Geisler, *J. Mater. Chem.*, 1995, **5**, 1861.
10 I. R. Whittall, M. G. Humphrey, M. Samoc, J. Swiatkiewicz and B. Luther-Davies, *Organometallics*, 1995, **14**, 5493; I. R. Whittall, M. P. Cifuentes, M. G. Mark, B. Luther-Davies, M. Samoc, S. Houbrechts, A. Persoons, G. A. Heath and D. C. R. Hockless, *J. Organomet. Chem.*, 1997, **549**, 127.
11 A. M. McDonagh, M. G. Humphrey, M. Samoc, B. Luther-Davies, S. Houbrechts, T. Wadw, H. Sasabe and A. Persoons, *J. Am. Chem. Soc.*, 1999, **121**, 1405.
12 A. Hidetomo, Y. Yasuhiko and M. Kazuhiro, *Jpn. Pat.*, 05273616, 1993.
13 Y. Xiong, X. H. Zou, J. Z. Wu, H. Y. Yang and L. N. Ji, *Synth. React. Inorg.*, *Met.-Org. Chem.*, 1998, **28**, 1445.
14 J. Z. Wu, L. Li, T. X. Zeng and L. N. Ji, *Polyhedron*, 1997, **16**, 103.
15 M. Sherk-Bahae, A. A. Said and E. W. Van Stryland, *Opt. Lett.*, 1989, **14**, 955.
16 M. Sherk-Bahae, A. A. Said, T. H. Wei, D. J. Hagan and E. W. Van Stryland, *IEEE J. Quantum Electron.*, 1990, **26**, 760.
17 A. A. Said, M. Sherk-Bahae, D. J. Hagan, T. H. Wei, J. Wang, J. Young and E. W. Van Stryland, *J. Opt. Soc. Am. B.*, 1992, **9**, 405.
18 P. A. Mabrouk and M. S. Wrighton, *Inorg. Chem.*, 1986, **25**, 526.
19 R. Hage, R. Prins, J. G. Haasnoot, J. Reedijk and J. G. Vos, *J. Chem. Soc.*, *Dalton Trans.*, 1987, 1389; R. Wang, J. G. Vos, R. H. Schmehl and R. Hage, *J. Am. Chem. Soc.*, 1992, **114**, 1964; E. M. Ryan, R. Wang, J. G. Vos, R. Hage and J. G. Haasnoot, *Inorg. Chim. Acta*, 1993, **208**, 49.
20 C. K. Johnson, ORTEP, Report ORNL-5138, Oak Ridge National Laboratory, Oak Ridge, TN, 1976.
21 M. A. Anderson, J. P. G. Richards, A. G. Stard, F. S. Stephens, R. S. Vagg and P. A. Williams, *Inorg. Chem.*, 1995, **25**, 4847.
22 J. Z. Wu, B. H. Ye, L. Wang, L. N. Ji, J. Y. Zhou, R. H. Li and Z. Y. Zhou, *J. Chem. Soc.*, *Dalton Trans.*, 1997, 1395.
23 B. H. Ye, X. M. Chen, T. X. Zeng and L. N. Ji, *Inorg. Chim. Acta*, 1995, **240**, 5.
24 D. P. Rillema, D. S. Jones, C. Woods and H. A. Levy, *Inorg. Chem.*, 1992, **31**, 2935.
25 J. Bueu and A. J. Stoll, *Acta Crystallogr.*, *Sect. C*, 1996, **52**, 1174.
26 E. E. Perez-Cordero, C. Campana and L. Echegoyen, *Angew. Chem.*, *Int. Ed. Engl.*, 1997, **36**, 137.
27 S. Zails and V. Drchal, *Chem. Phys.*, 1987, **118**, 313.
28 K. M. Iwamura, *Nippon Kagaku Kaishi*, 1983, **10**, 1456.
29 L. Yang, R. Dorsinville, Q. Z. Wang, P. X. Ye, R. R. Alfano, R. Zamboni and C. Taliani, *Opt. Lett.*, 1992, **17**, 323.
30 Z. R. Chen, H. W. Hou, X. Q. Xin, K. B. Yu, H. C. Zeng and S. Shi, *J. Phys. Chem.*, 1995, **99**, 8717.
31 S. Shi, H. W. Hou and X. Q. Xin, *J. Phys. Chem.*, 1995, **99**, 4050.
32 S. Guha, C. C. Frazier, P. L. Porter, K. Kang and S. E. Finberg, *Opt. Lett.*, 1989, **14**, 952.
33 W. J. Blau, H. J. Byrne, D. J. Cardin and A. P. Davey, *J. Mater. Chem.*, 1991, **1**, 245.
34 J. S. Shirk, J. R. Lindle, F. J. Bartoli, Z. H. Kafafi and A. W. Snow, in *Materials for Nonlinear Optics*, eds. S. R. Marder, J. E. Sohn and G. D. Stucky, American Chemical Society, Washington, 1992, p. 626.
35 Y. Wang and L. T. Cheng, *J. Phys. Chem.*, 1992, **96**, 1530.
36 G. M. Sheldrick, SHELXS-97, Program for structure solution, University of Göttingen, 1997.

Paper 9/05790K